Photophysical Properties of 1,3,5-Tris(2-naphthyl)benzene and Related Less-Arylated Compounds: Experimental and Theoretical Investigations†

Gianfranco Bocchinfuso,‡ Claudia Mazzuca,‡ Antonio Palleschi,*,‡ Roberto Pizzoferrato,§ and Pietro Tagliatesta‡

Department of Chemical Science and Technologies, University of Rome-Tor Vergata, Via della Ricerca Scientifica, 00133-Rome, Italy, and Department of Mechanical Engineering, University of Rome-Tor Vergata, Via del Politecnico 1, 00133 Rome, Italy

Received: May 29, 2009; Revised Manuscript Received: July 8, 2009

Recently, a growing interest has concerned compounds characterized by high chemical and photophysical stability and high quantum yield for their possible technological applications. 1,3,5-Tris(2-naphthyl)benzene (N3B), 1,3-bis(2-naphthyl)benzene (N2B), and 2-naphthyl-benzene (N1B) are promising compounds, but they needed a detailed photophysical characterization. In this context, theoretical and experimental investigations have been carried out. Steady-state and decay time fluorescence measurements indicate that the second naphthyl group, added in the meta position of N1B, perturbs the electronic levels, whereas the further naphthyl addition, leading to N3B, does not promote changes in all of the observed properties. The investigated compounds show a biexponential fluorescence decay that has been attributed to a rearrangement involving the exited states S_1 and S_2. The minimum structure corresponding to the S_1 and S_2 states has been obtained at the configuration interaction with single excitations (CIS) level of theory. For the ground-state geometry, a conformational analysis at the Hartree−Fock level has also been carried out. We have evaluated the energy gaps between electronic levels by using Zerner's intermediate neglect of differential overlap (ZINDO) method. The species involved in the fluorescence have been experimentally characterized, and the decay-associated spectra have been obtained.

Introduction

Polycyclic aromatic hydrocarbons (PAHs) have been extensively studied for their interesting properties and applications. Many of them, having high molecular weights, are good models of the structure of graphite[1] and are synthesized through a few steps starting from simple halogenated aromatic compounds and functionalized boronic acids by the Suzuki coupling reaction.[2] PAHs with low molecular weights are used for building OLEDs and WOLEDs[3] and represent a class of fluorescent compounds with promising properties in the field of industrial applications. Furthermore, some of the simplest PAH compounds are well studied because they form organic glass materials.[4] During the investigations of some of us on the catalytic properties of the metalloporphyrins, it was found that arylethynes are able to undergo cyclodimerization and cyclotrimerization reactions, depending on the catalyst and the substrate, giving heterobiaryls and tetraryls, respectively.[5] In particular, our attention was attracted to the interesting properties of 1,3,5-tris(2-naphthyl) benzene (N3B), which was obtained by the cyclotrimerization reactions of 2-ethynylnaphthalene catalyzed by cobaltocene or by the Suzuki coupling of 1,3,5-tribromobenzene and 2-naphthalene boronic acid. The compound N3B has been investigated in the past decade, for example, for its propensity to form glassy phases,[4,6] but a thorough insight into its spectroscopic behavior is not available yet.

In this work, the photophysical properties of N3B and related less-arylated compounds, 2-naphthyl-benzene (N1B) and 1,3-bis(2-naphthyl)benzene (N2B), have been investigated (Scheme 1). The synthesis and properties of N2B, to the best of our knowledge, were never reported in the literature.

SCHEME 1

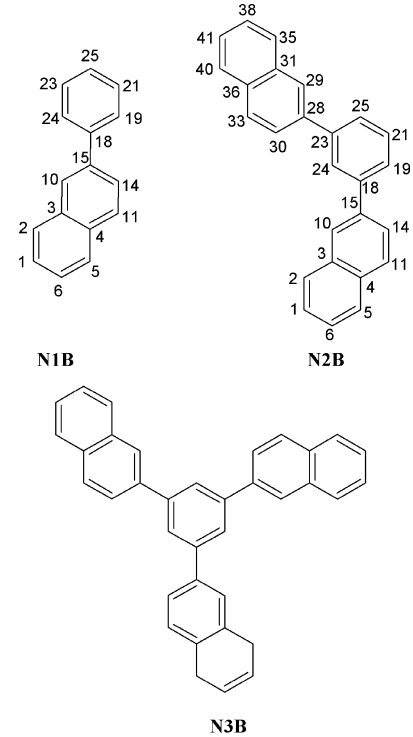

Among these three compounds, only N1B has previously been investigated[7] from spectroscopic and theoretical points of view.

† Part of the "Vincenzo Aquilanti Festschrift".

* Corresponding author. E-mail: antonio.palleschi@uniroma2.it.
‡ Department of Chemical Science and Technologies.
§ Department of Mechanical Engineering.

10.1021/jp905059v
Published on Web 08/14/2009

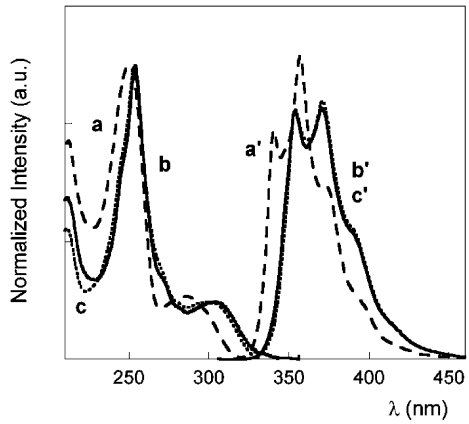

Figure 1. Absorption (a, b, c) and emission (a′, b′, c′) spectra of N1B (a, a′, dashed line), N2B (b, b′, continuous line), and N3B (c, c′, dotted line) in acetonitrile. Absorption spectra are normalized with respect to the value at the absorption maximum, whereas emission spectra are normalized to the unit area (λ_{ex} = 298 nm).

As reported in the literature, the N1B fluorescence emission can be rationalized by assuming a large conformational rearrangement that takes place in the electronic excited state (S_1). In the ground state (S_0), phenyl and naphthyl rings are twisted, whereas in the S_1 state, they assume a roughly coplanar conformation. Furthermore, it has been pointed out that a direct transition, between the electronic states S_0 and S_1, is forbidden, and slightly higher energy excited states are populated after light absorption. Next, the molecule relaxes nonradiatively to the S_1 state and then radiatively to S_0; the role of higher excited states (S_2, S_3, etc.) in the fluorescence properties of N1B has been poorly investigated.

A detailed knowledge of the spectroscopic features of N1B, N2B, and N3B is of interest because they belong to a new class of compounds useful to be applied, for example, in OLED construction owing to their high quantum yields (Table 1) and stability. Recently, they have also been used as compounds in multicomponent organic systems for up-conversion-induced delayed fluorescence.[8] Furthermore, chemical groups can be easily added to these compounds to tune their photophysical properties opportunely. In this context, a theoretical approach, able to predict their conformational and spectroscopic features, will be useful in the design of new derivatives.

A spectroscopic and theoretical characterization of these compounds will be reported and discussed in this article.

Experimental Section

Materials. Silica gel 60 (70−230 and 230−400 mesh, Merck) was used for column chromatography. High-purity-grade nitrogen gas was purchased from Rivoira. All other reagents were from Fluka Chem., Aldrich Chem., or Carlo Erba and were used as received. Solvents were of spectroscopic grade.

1,3,5-Tris(2-naphthyl)benzene and 2-Naphthyl-benzene. N3B and N1B were synthesized as reported in the literature.[4]

1,3-Bis(2-naphthyl)benzene. 1,3-dibromobenzene (1g, 4.2 mmol) was dissolved in 30 mL of toluene, and after that naphthalene-2-boronic acid (2.16 g, 12.6 mmol) was added. PPh_3 (40 mg, 0.15 mmol) and 5 mL of 2 M sodium carbonate solution were added to the mixture, which was then deareated for 20 min with a stream of argon. $Pd(CH_3CO_2)_2$ (20 mg, 0.09 mmol) was added, and the solution was refluxed for 4 h under nitrogen. The solvent was evaporated, and the residue was purified by silica gel column eluting with a diethyl ether/petroleum ether (0.3:99.7, 70% yield). The EI-MS molecular weight was 330 (M+). Anal. Calcd for $C_{26}H_{18}$: C, 94.51; H, 5.49. Found: C, 94.60; H, 5.47. ^{1}H NMR ($CDCl_3$, δ): 8.2 (s, 2H), 8.14 (s, 1H), 7.97 (m, 8H), 7.79 (d, 2H, J = 8 Hz), 7.57 (m, 5H).

Methods. ^{1}H NMR spectra were recorded as $CDCl_3$ solutions on a Bruker AM-300 instrument using residual solvent signal as an internal standard. GC-mass spectra were recorded on a VG-4 spectrometer equipped with a 30 mt Supelco SPB-5 capillary column. UV−vis absorption spectra were recorded with a Varian 100 scan UV/vis spectrophotometer (Varian Inc., Palo Alto, CA). Steady-state fluorescence spectra were measured on a Fluorolog spectrofluorimeter (Horiba, Japan). Time-resolved experiments were performed on a CD900 single photon counting apparatus (Edinburgh Instruments, Edinburgh, U.K.). Nanosecond pulsed excitation was obtained with a flash lamp filled with ultrapure hydrogen (0.3 bar, 40 kHz repetition rate; instrument pulse width: 1.2 ns). When possible, time-resolved experiments were performed on a Lifespec-ps Instruments Edinburg instrument (U.K.) operating in single photon counting mode. Nanosecond pulse excitation was obtained with a NanoLED light source (298 nm, pulse excitation width: 1.0 ns 0.9 MHz repetition rate). Fluorescence intensity decays were acquired until a peak value of 10^4 counts was reached and analyzed with the software provided by Edinburgh Instruments.

The decay curves were fitted by a nonlinear least-squares analysis to exponential functions through an iterative deconvolution method. In particular, the decays were fitted according to the expression

$$I(t) = \sum_i \alpha_i \exp(-t/\tau_i) \quad (1)$$

where τ_i is the ith decay time observed and α_i is the ith preexponential factor that represents the relative contribution of the decay to the emission intensity. The obtained results are unaffected by the use of different methods of fitting, such as global fit or distribution analysis.[9−11]

Spectral components associated with the individual decay time (DAS) were obtained by analysis of the decay curves measured at different emission wavelengths (λ_{em}).[10,12] In particular, the fluorescence intensity, at different wavelengths ($F_i(\lambda)$), of the ith species (with decay time τ_i) was calculated to be

$$F_i(\lambda) = F(\lambda) f_i(\lambda) \quad (2)$$

where $F(\lambda)$ is the fluorescence intensity of the steady-state spectrum, and $f_i(\lambda)$ is the fractional contribution of each component in the multiexponential decay to the total emission calculated according to

$$f_i(\lambda) = \alpha_i(\lambda)\tau_i / \sum_i \alpha_i(\lambda)\tau_i \quad (3)$$

From these data, quantum yields and emissive and nonradiative decay rate constants for each component of the total emission spectra were obtained.

Fluorescence experiments were carried out in quartz cells using solutions bubbled for 20 min with ultrapure argon before each measurement. We obtained the quantum yield by using a solution of 2-aminopyiridine in 0.1 N sulfuric acid as a fluorescence standard.[13] Excitation and emission spectra were corrected for the instrument responses. Temperature was controlled within ±0.1 °C with a thermostatted cuvette holder.

The solvents used (acetonitrile, tetrahydrofuran, and cyclohexane) span a wide polarity range in terms of both different

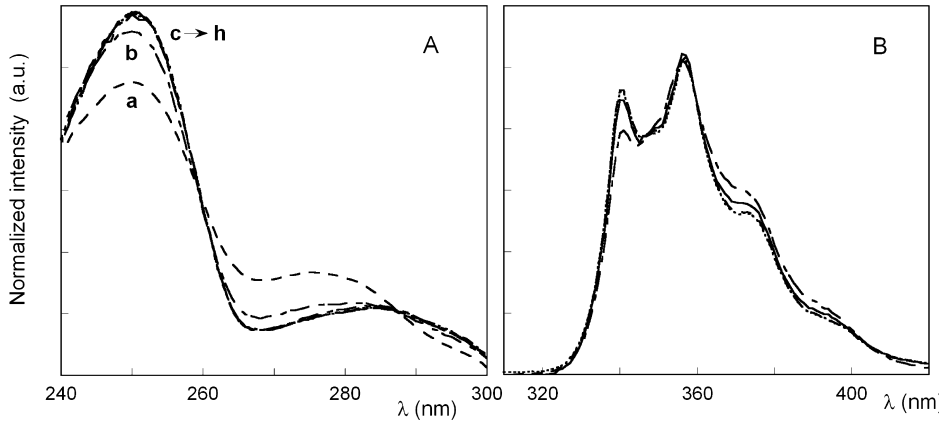

Figure 2. Excitation (panel A) and emission (panel B) spectra of N1B in acetonitrile. The emission wavelengths for the excitation spectra are (a) 320, (b) 325, (c) 330, (d) 340, (e) 350, (f) 370, (g) 390, and (h) 410 nm, respectively, whereas the excitation wavelengths for the emission spectra are 285 (dashed line), 298 (dotted line), 310 (straight line), and 320 nm (dotted dashed line).

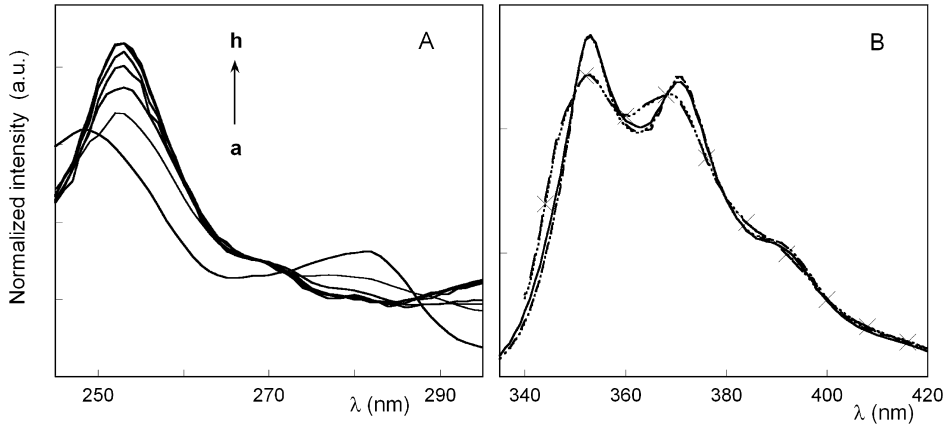

Figure 3. Excitation (panel A) and emission (panel B) spectra of N2B in acetonitrile. The emission wavelengths for the excitation spectra are (a) 320 nm, (b) 330 nm, (c) 335 nm, (d) 340 nm, (e) 350 nm, (f) 370 nm, (g) 390, and (h) 410 nm, respectively, whereas the excitation wavelengths for the emission spectra are 285 (straight line), 298 (dashed line), 310 (dotted line), 330 (dotted dashed line), and 335 nm (dashed line and crosses).

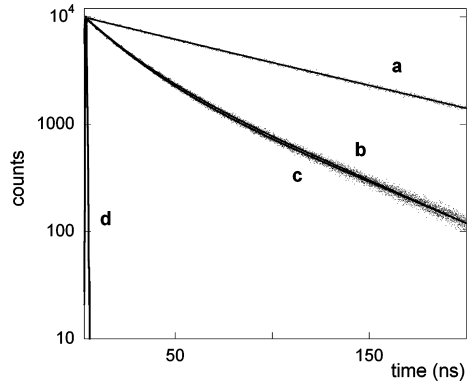

Figure 4. Decay profile (λ_{ex} = 298 nm) for (a) N1B, (b) N2B, and (c) N3B (λ_{em} = 356 nm for a and 370 nm for b and c). The full lines represent the best fit to the experimental data. (d) Lamp profile.

TABLE 1: Fluorescence Quantum Yields and Emission Maximum Wavelengths ($\lambda_{em,max}$) of N1B, N2B, and N3B in Solvents at Different Polarity[a]

sample	solvent	quantum yield	$\lambda_{em,max}$ (nm)		
N1B	acetonitrile	0.35 ± 0.03	341	357	374
	tetrahydrofuran	0.25 ± 0.02	341	357	374
	cyclohexane	0.30 ± 0.01	348	357	374
N2B	acetonitrile	0.51 ± 0.04	353	371	391
	tetrahydrofuran	0.39 ± 0.04	354	372	393
	cyclohexane	0.37 ± 0.03	348	365	391
N3B	acetonitrile	0.37 ± 0.03	354	371	393
	tetrahydrofuran	0.36 ± 0.03	354	372	393
	cyclohexane	0.33 ± 0.03	348	367	390

[a] λ_{ex} = 298 nm.

orientation polarizability (Δf_p)[10,14] and empirical "*py* scale".[15] Δf_p was obtained by the static dielectric constant (ε) and refractive index (n) of the solvent by means of the following equation

$$\Delta f_p = (\varepsilon - 1)/(2\varepsilon + 1) - (n^2 - 1)/(2n^2 + 1) \quad (4)$$

The empirical *py* scale of solvent polarity has been established on the basis of the emission response of pyrene. The Δf_p and the *py* values are 0.31 and 1.70; 0.21 and 1.27; and 0.00 and 0.56 for acetonitrile, tetrahydrofuran, and cyclohexane, respectively.

Theoretical Calculations. The structure of S_0 was optimized at the ab initio Hartree−Fock (HF) level of theory. The geometries of S_1 and S_2 were optimized at the configuration interaction with single excitations (CIS)[16] level. In all cases, the 6-31+G(d) basis set was used. For quantitative comparisons of the calculated absorption and emission energies with the experimental values, both the ab initio CIS method and the semiempirical Zerner's intermediate neglect of differential overlap (ZINDO) method[17] were used. All calculations were carried out by means of the GAUSSIAN 03 program.[18]

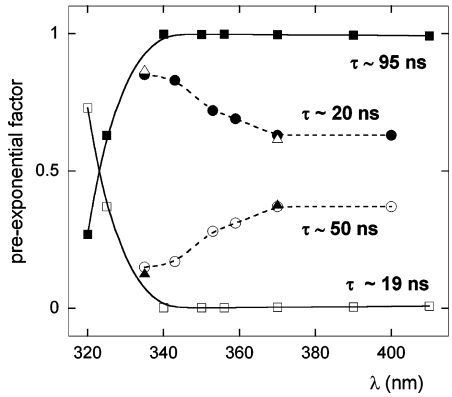

Figure 5. Pre-exponential factors, determined from time-resolved fluorescence data in acetonitrile, for N1B (squares), N2B (circles), and N3B (triangles) versus the emission wavelength (λ_{ex} = 260 nm). The pre-exponential factors associated with short decay times are represented by □, ●, and ▲ for N1B, N2B, and N3B, respectively. Lines are only a guide for the eyes. The uncertainty in the pre-exponential factors is around 10%.

Results

Spectroscopic Data. As shown in Figure 1, the UV absorption of N1B in acetonitrile is characterized by three spectral bands in the 200−340 nm region, with λ_{max} = 286, 250, and 212 nm and $\varepsilon/10^4 = (1.38 \pm 0.11)$, (6.02 ± 0.07), and (4.35 ± 0.50) M^{-1} cm^{-1}, respectively. The emission spectrum displays a structured profile whose peaks are at 341, 357, and 374 nm, with a quantum yield of 0.35, which is in agreement with previously published data.[7]

The absorption and emission spectra of N2B (Figure 1) reveal that the addition of a naphthyl group to position three of the phenyl moiety (meta addition) perturbs the spectroscopic features with respect to N1B. In particular, the ^1B_b band of N1B (∼250 nm) results red-shifted about 4 nm, whereas a more consistent red shift of ∼14 nm for the ^1L_a band (∼300 nm) is observed. This result indicates that the major effect on the electronic structure, on passing from N1B to N2B, implies an increase in the conjugation in the transversal direction (short axis of naphthyl group).[19]

The fluorescence spectrum of N2B is red-shifted, with respect to N1B, by ∼14 nm, and a different relative intensity of peaks is observed. Interestingly, the addition of a third naphthyl group to meta position (N3B) does not promote further changes with respect to N2B, with the absorption and fluorescence spectra of N2B and N3B practically superimposed.

To rationalize these photophysical results, we have performed a combination of steady-state and time-resolved fluorescence experiments by varying experimental parameters such as solvent polarity, temperature, and excitation and emission wavelengths.

Figures 2 and 3 report the results from steady-state experiments at different excitation and emission wavelengths[20] for N1B and N2B, respectively. Because of the great similarity of N3B and N2B, the experimental data obtained for the former compound have not been reported. As shown in Figures 2A and 3A, by acquiring the excitation spectra at lower emission wavelengths, a blue shift is observed (more evident for the band at about 280 nm). In the emission spectra (Figures 2B and 3B), a trend with the excitation wavelength is not clear, but a general rearrangement of the vibronic structures is well evident.

Figure 4 reports the time-resolved fluorescence data of the three compounds in acetonitrile, acquired exciting close to the absorption maximum, and monitoring the emission at the wavelength corresponding to the fluorescence maxima. N2B and N3B show superimposed profiles, and, at a glance, their decay is faster compared with that of N1B. The fitting of the data according to eq 1 shows that all three compounds display biexponential trends but with a different relative weight of the two species involved in the fluorescence. In particular, in N2B and N3B, the two species contribute similarly; on the contrary, in N1B, the species with longer decay time (τ_1) dominates (Table 2).

Time-resolved fluorescence experiments at different emission wavelengths (λ_{em}) have also been carried out in acetonitrile. In all cases, τ_1 and τ_2 remain very close to the values reported in Table 2 (about 95 and 19 ns for N1B and about 50 and 20 ns for N2B and N3B). On the contrary, the relative weights of the emitting species change; in particular, the contributions associated with the shorter decay time (τ_2) increase when the fluorescence decay is monitored at lower emission wavelengths, particularly for N1B, where it increases from 0.01 (at 356 nm) to 0.73 (at 320 nm). These results are summarized in Figure 5, where the pre-exponential factors, for the different species detected for N1B, N2B, and N3B, are reported.

The DAS analysis has been applied to N1B and N2B. The fluorescence spectra obtained for longer and shorter time decay species are reported in Figure 6, and the relative quantum yields and radiative and nonradiative rate constants are reported in Table 3. The major differences between the two compounds are due to the species with shorter decay time mainly in the higher energy region, and a dramatic difference of the quantum yields is obtained. On the contrary, the species with longer decay time are very similar, except for a blue shift observed in the spectrum of N1B with respect to N2B that parallels the results obtained with steady-state fluorescence.

In the case of N2B, fluorescence decay experiments have been performed by changing the excitation wavelength (λ_{ex}) (data not shown). The relative weight of the species with the shorter time increases from 0.62 to 0.90 at λ_{ex} = 285 and 330 nm, respectively. In summary, the species at shorter decay time seem to prevail with exciting at lower energy and monitoring at higher energy.

The sensitivity of the emission spectra to solvent polarity has also been analyzed. As an example, in Figure 7, the emission spectra of N1B and N2B in different solvents (acetonitrile, tetrahydrofuran, and cyclohexane) are reported. In N2B, slight blue shifts of the peaks at about 356 and 374 nm, without significant changes in the relative intensities, are observed in cyclohexane. (Also see Table 1.) In the case of N1B, a general reorganization of the band structure has been obtained, involving the relative peak intensities and the λ_{max} of the higher energy band. The absorption spectra (not shown) are not strictly influenced by solvent polarity.

Furthermore, time-dependent fluorescence experiments have been carried out in acetonitrile, tetrahydrofuran, and cyclohexane (Table 2). In all cases, an increase in τ_1 is observed in cyclohexane, whereas slight effects have been detected for τ_2.

Finally, time-resolved fluorescence experiments at different temperature (from 280 to 340 K) have been performed. Figure 8 reports the pre-exponential factors associated with the two decay times for N2B. The values of the two decay times are unaffected by the temperature.

Computational Data. The main differences of the spectroscopic behavior have been detected by the addition of one naphthyl group in the meta position of N1B. For this reason, ab initio calculations on N1B and N2B have been performed.

We have carried out conformational analyses of the ground state of N1B and N2B at the HF level, using the 6-31+G(d)

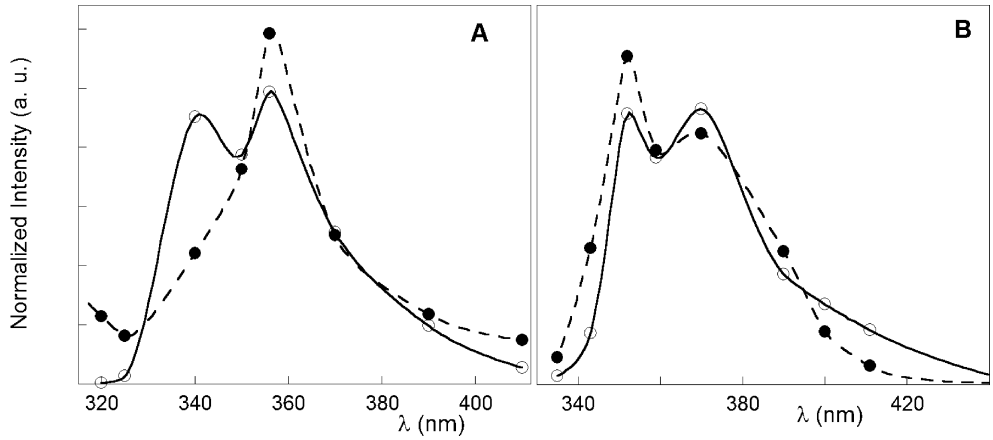

Figure 6. Normalized decay-associated spectra (DAS) of the shorter (dashed line, ●) and longer (continuous line, ○) time decay species of N1B (panel A) and N2B (panel B) in acetonitrile. Spectra are normalized to unit area.

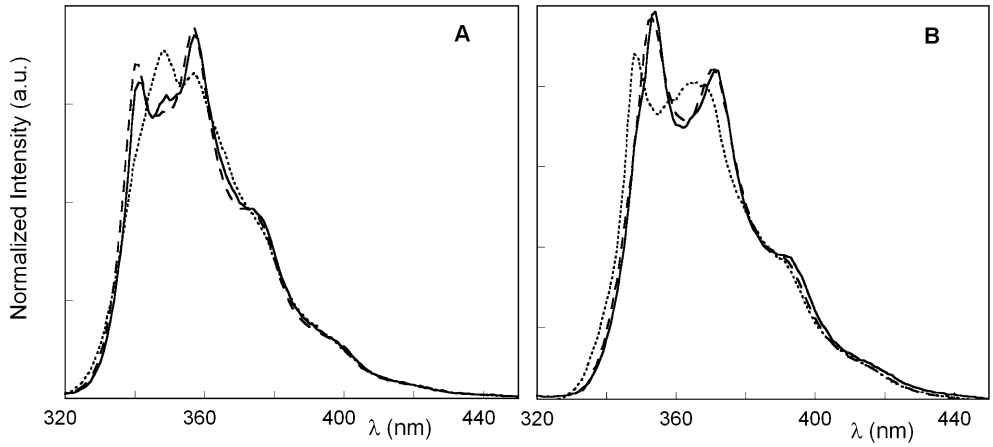

Figure 7. Absorption and fluorescence spectra of N1B (panel A) and N2B (panel B) in acetonitrile (dashed line), tetrahydrofuran (continuous line), and cyclohexane (dotted line). Fluorescence spectra are normalized to the unit area (λ_{ex} = 298 nm).

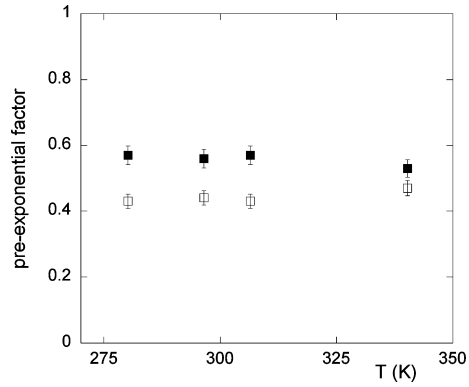

Figure 8. Pre-exponential factors for N2B determined from time-resolved fluorescence experiments as a function of the temperature corresponding to the decay time: ~20 (■) and ~50 ns (□).

TABLE 2: Time-Dependent Fluorescence Parameters for the Three Samples in Different Solvents[a,b,c]

sample	solvent	α_1	τ_1 (ns)	f_1	α_2	τ_2 (ns)	f_2	χ^2
N1B	acetonitrile	0.93	98	0.99	0.07	19	0.01	1.0
	THF	0.96	82	0.99	0.04	11	0.01	1.1
	cyclohexane	0.95	120	0.99	0.05	20	0.01	1.1
N2B	acetonitrile	0.37	53	0.59	0.63	21	0.41	1.2
	THF	0.34	67	0.65	0.66	19	0.35	1.3
	cyclohexane	0.26	88	0.57	0.74	23	0.43	1.1
N3B	acetonitrile	0.38	56	0.63	0.62	20	0.37	1.2
	THF	0.33	70	0.60	0.67	21	0.40	1.3
	cyclohexane	0.25	94	0.55	0.75	25	0.45	1.3

[a] λ_{ex} = 298 nm; λ_{em} = 356 nm for N1B and 370 nm for N2B and N3B. [b] Uncertainty in decay times is around 5%, whereas the uncertainty in the pre-exponent and in the fluorescence fraction is around 10%. [c] From eqs 1 and 3.

basis set, by changing the dihedral angles (ϕ) between the phenyl and naphthyl rings; the structural parameters for the energy minimum conformations are reported in Table 4.

The N1B minimum presents a ϕ value equal to −46.5° (or +46.5° in the corresponding symmetric isomer). Minimizations of N1B with ϕ constrained to 0 and 90° have shown energies of 3.3 and 1.6 kcal/mol higher with respect to the minimum, respectively. These values define the rotational barriers of the ϕ dihedral.

In the case of N2B, two dihedral angles characterize the relative orientation of phenyl and naphthyl rings (ϕ_1 and ϕ_2). In principle, the relative minima, obtainable by combination of positive and negative values of ϕ_1 and ϕ_2, are not equivalent. However, our conformational analysis has shown that they are practically isoenergetic (difference <0.1 kcal/mol).

It is noteworthy that the torsional angles of N2B in the deepest energy minimum, −45.2 and 44.5°, are close to those obtained for N1B. (See Table 4.) Also, the rotational barriers, for the two angles, are nearly unchanged after the addition of the second naphthyl group.

To obtain the minimum structure for the excited states, S_1 and S_2, we have used the CIS approach with the 6-31+G(d) basis set; Table 3 reports the obtained structural parameters for N1B and N2B.

TABLE 3: Kinetic and Photophysical Parameters of the Two Species of N1B and N2B in Acetonitrile[a]

	τ_2 (~20 ns)			τ_1 (~50−100 ns)		
sample	quantum yield	k_r (10^6 s^{-1})[b]	k_{nr} (10^6 s^{-1})[b]	quantum yield	k_r (10^6 s^{-1})[b]	k_{nr} (10^6 s^{-1})[b]
N1B	0.34	3.5	6.7	0.010	0.53	52
N2B	0.29	5.5	13	0.22	10	37

[a] Uncertainty in the values is around 20%. [b] k_r and k_{nr} are the radiative and nonradiative decay rate constants, respectively.

It is well known that the CIS approach poorly predicts the energy gap between electronic levels.[21] This has been confirmed in the case of N1B and N2B (data not shown). Therefore, for a quantitative comparison with experimental absorption and fluorescence data, the ZINDO method has been used, which is known to reproduce them with a reasonable accuracy if used with reliable conformations.[21] For the known deficiency of ZINDO to be applied in optimization procedures, the minimum structures, obtained at HF (ground state) and CIS (excited states) levels, have been used. The predicted absorption wavelengths, the relative oscillator strength, f_{osc}, and the main contributions to each transition are reported in Table 5 for N1B and in Table 6 for N2B. In regard to the fluorescence, only the gap between the excited states (S_1 and S_2) and the ground state S_0 is reported.

The general profiles for the calculated absorption of N1B and N2B are similar. In both cases, the first transition (at about 315 nm) is forbidden, whereas absorption at about 290 and 260 nm is predicted to be more intense. As a general rule, few bands in N2B (roughly corresponding to the predicted absorption bands for naphthalene) split into two signals compared with those of N1B. As an effect, this produces a general red shift of the absorption spectrum, particularly for the transition predicted at 296 and 301 nm (corresponding to the band at 296 nm for N1B). The predicted gap $S_1 \rightarrow S_0$ and $S_2 \rightarrow S_0$ profiles appear to be similar for the two compounds; a slight red shift is obtained for $S_1 \rightarrow S_0$ in the case of N2B.

Discussion

In this article, three arylated benzenes (N1B, N2B, and N3B) have been analyzed by means of spectroscopic and theoretical approaches.

First of all, the effects produced by the addition of naphthyl groups to meta positions of N1B have been analyzed. The comparison between the steady-state and time-resolved fluorescence data (Figures 1 and 4 and Table 1) indicates that the introduction of a second naphthyl group to N1B perturbs the electronic states of the molecule. Surprisingly, the further addition of another naphthyl group, leading to N3B, does not introduce substantial changes. As a general rule, under all properties investigated by us, N2B and N3B are indistinguishable.

From time-resolved fluorescence experiments, the analyzed compounds show biexponential decays (Table 2). This is in contrast with the data previously reported for N1B,[7c] where only a decay time was used to fit the decay time profile. For this reason, this case will be better discussed. By adopting a biexponential function instead of a monoexponential function to fit the N1B decay time data, we observe an improvement in the χ^2 value from 1.2 to 1.0. In a similar way, the presence of two emitting species for N1B is also observed with changing the decay time experimental conditions. In particular, the species with shorter decay time becomes dominant when the fluorescence is monitored at $\lambda_{em} < 340$ nm (Figure 5). Furthermore, the dependence of the absorption and steady-state fluorescence spectra that is observed in N1B with changing solvent polarity (Figure 7) could be explained by considering two different emitting species, as already suggested in analogous cases.[15]

The two emitting species in N1B and N2B have been further characterized by means of DAS analysis. Using this approach the fluorescence spectra, the quantum yields, and the radiative and nonradiative decay rate constants for the species involved in the emission have been obtained. In both cases, the species with the shorter decay time present a blue shift in the emission spectra. This trend is particularly evident in N1B, where the high energy peak, not well resolved, seems to be shifted by tens of nanometers at higher energies. As a result, for both N1B or N2B, in the high-energy region, the shorter time species dominate.

The existence of two emitting species could be due to different factors deriving from both ground- (different isomers, aggregation, etc.), or excited- (solvent relaxation, charge separation, conformational rearrangements, coupling between excited states, etc.) state phenomena.[20,22−26]

The absence of significant changes in the time-resolved fluorescence experiments as a function of concentration (data not shown) rules out the presence of aggregates in the range investigated (1−100 μM).

The role of different ground-state conformers has also been analyzed by means of a conformational analysis performed on N1B and N2B. As a result, the rotation around the torsional angle between the naphthyl and phenyl moieties is possible at room temperature. The conformation corresponding to the maximum hindrance, with the two groups roughly planar, is about 3.3 kcal/mol higher than the minimum characterized by a ϕ value of about 45°. Such results nicely recall those obtained using a similar approach on biphenyl.[27] As pointed out by the author, the uncorrelated HF theory efficiently predicts the structural parameters of the absolute minimum, but, lacking the electron correlation terms, overestimates the energetic cost of planar conformation (3.3 kcal/mol predicted against an experimental value of 1.4 ± 0.5). Paralleling these results, the obtained rotational barrier for N1B and N2B can be considered to be an upper limit; reasonably, a value <2 kcal/mol should be reliable. Similar prediction has been proposed on the basis of the molecular mechanics calculation on N3B.[6a] At room temperature, this means that (i) the different conformers can easily interconvert, and (ii) a non-negligible fraction of molecules populates, in the ground state, conformations with coplanar phenyl and naphthyl rings.

The two N1B minima are equal for symmetry, so the observed biexponential decay is not a consequence of ground-state conformers. For N2B, the two minima, characterized by a different orientation of the phenyl and naphthyl rings (i.e., about (45°, 45) and (45, −45)), could be different. However, our calculations indicate that these minima are almost isoenergetic and their spectroscopic features, obtained at the CIS level (data not shown), are nearly coincident. These data are not consistent with two emitting species with different decay times and populations. In addition, the similarity with N1B supports this point of view, as well as the evidence of the statistical weights of the two species in N2B, in the fluorescence decay, being unaffected by changing the temperature.

For all of these reasons, excited-state effects must be considered to explain the photophysical behavior of the compounds under investigation. An attempt to further characterize the excited species can be done by performing fluorescence

TABLE 4: Structural Parameters Obtained from Ab initio Calculations for S_0, S_1, and S_2 Electronic Levels for N1B and N2B

atoms involved[a]	bonds (nm)						
	N1B			N2B			
	value (S_0)	value (S_1)	value (S_2)	value (S_0)	value (S_1)	value (S_2)	
1−2	0.136	0.137	0.139	1.36	1.36	0.139	naphthalene ring - 1
2−3	0.142	0.143	0.140	1.42	1.42	0.140	
3−4	0.141	0.144	0.148	1.41	1.41	0.148	
4−5	0.142	0.139	0.141	1.42	1.42	0.141	
5−6	0.136	0.139	0.139	1.36	1.36	0.139	
6−1	0.142	0.140	0.141	1.42	1.42	0.141	
3−10	0.142	0.139	0.140	1.42	1.42	0.140	
10−15	0.137	0.145	0.140	1.36	1.36	0.140	
15−14	0.143	0.143	0.142	1.42	1.43	0.142	
14−11	0.136	0.136	0.139	1.36	1.36	0.139	
11−4	0.142	0.144	0.140	1.42	1.42	0.140	
15−18	0.149	0.143	0.147	1.49	1.49	0.147	
18−19	0.139	0.143	0.140	1.39	1.41	0.140	benzene ring
19−21	0.139	0.137	0.138	1.38	1.39	0.138	
21−25	0.139	0.140	0.139	1.39	1.38	0.139	
25−23	0.139	0.139	0.139	1.39	1.43	0.139	
23−20	0.139	0.138	0.138	1.38	1.43	0.139	
20−18	0.139	0.143	0.140	1.39	1.37	0.140	
23−28				1.54	1.43	0.149	
38−35				1.37	1.37	0.136	naphthalene ring - 2
35−31				1.42	1.43	0.142	
31−36				1.42	1.44	0.141	
36−40				1.42	1.39	0.142	
40−41				1.37	1.39	0.136	
41−38				1.42	1.40	0.142	
31−29				1.42	1.39	0.142	
29−28				1.37	1.45	0.137	
28−30				1.42	1.43	0.142	
30−33				1.37	1.36	0.136	
33−36				1.42	1.44	0.142	
	dihedrals (deg)						
	N1B			N2B			
10−15−18−20	−46.5	−3.3	−31.0	−45.2	49.31	30.5	dihedral-1
29−28−23−25				44.5	−3.4	−46.7	dihedral-2

[a] Numbering of the atoms is indicated in Scheme 1.

TABLE 5: Absorption and Emission Parameters Calculated at ZINDO Level for N1B

nm	f_{osc}	main contribution[a]
		Absorption
314	0.0045	H → L + 1 (49%)
296	0.1656	H → L (84%)
271	0.0050	
259	1.2837	H-1 → L (44%) and H → L + 1 (38%)
234	0.6169	H-1 → L + 1 (60%)
233	0.4468	H → L + 3 (30%) and H → L + 4 (30%)
230	0.2167	H → L + 4 (31%)
227	0.0102	
216	0.0502	
214	0.3982	H → L + 2 (49%)
208	0.0392	
207	0.0343	
		Emission S_1 Optimized Structure
357	0.6634	L → H (96%)
		Emission S_2 Optimized Structure
324	0.1979	L + 1 → H (48%) L → H-1 (35%)

[a] H and L indicate Homo and Lumo levels, respectively.

TABLE 6: Absorption and Emission Parameters Calculated at ZINDO Level for N2B

nm	f_{osc}	main contribution[a]
		Absorption
318	0.0047	H-3 → L (22%)
313	0.0059	H-1 → L + 3 (20%) and H → L + 1 (20%)
301	0.1367	H → L (51%)
296	0.1930	H-1 → L + 2 (43%) and H → L + 2 (37%)
280	0.037	
261	2.5432	H-2 → L +2 (32%) and H-1 → L + 3 (32%)
259	0.5834	H → L + 2 (27%)
235	0.1164	
234	0.2682	
233	0.2986	
230	0.8965	H-1 → L + 7 (20%)
229	0.2024	
		Emission (S_1 Optimized Structure)
359	0.7748	L → H (97%)
		Emission (S_2 Optimized Structure)
324	0.1921	L+2 → H (47%) and L → H-2 (35%)

[a] H and L indicate Homo and Lumo levels, respectively.

spectra in solvents at different polarity and by means of theoretical studies.

The electronic features of the emitting state are related to the fluorescence changes detected in the solvent at different polarity. According to the Lippert−Mataga equation,[9,14,22] the small shift in the fluorescence bands observed in the solvent with different polarity (Figure 7) rules out significant changes of the dipolar moment (i.e., charge transfer) in the emitting state taking place.

The solvent polarity affects the structure of the emission bands. This effect, already observed in similar compounds,[15] has been attributed to the extent of vibronic coupling between the weakly allowed first excited state and the strong allowed second excited singlet state.

Furthermore, as already mentioned, the emitting species, characterized by the shorter decay time, dominate the fluorescence detected at higher energy and, for N2B, the species with shorter decay time also becomes predominant if the excitation wavelength is close to 330 nm. In other words, in the region where absorption and fluorescence overlap (without Stoke shift), almost only one species, characterized by the shorter decay time, is present.

Ab initio investigations of the photophysical properties of N1B and N2B have been carried out. The simulations of absorption spectra have been performed using the semiempirical ZINDO approach on the minimum ground-state structure obtained after HF minimizations. The results can be summarized as: (i) for N1B, the data are in excellent agreement with the experimental values, showing, in the spectral region under investigation, bands with significant dipole transitions centered at 296, 259, 234, and 214 nm; (ii) the addition of a second naphthyl group does not change the general profile; (iii) some bands split and, according to experimental data, a red shift is observed, especially in the low-energy region of spectrum; and (iv) in both cases, the transition $S_0 \rightarrow S_1$ is forbidden and a more intense absorption is predicted to the second excited level.

To get insight into the role of the excited states, S_1 and S_2, the minimum structures corresponding to these levels for N1B and N2B have been obtained. To the best of our knowledge, computational data are available only for the S_1 level of N1B.[7]

From the data reported in Table 4, the S_1 state of N2B could be seen roughly as a chimera of the N1B structures in the S_0 and S_1 states. In a similar way, S_2 of N2B seems to be a chimera of S_0 and S_2 states of N1B. In other words, the excitation mainly affects a part of the molecule (the phenyl moiety and only one of two naphthyl groups), whereas the naphthyl group not involved in the transition retains the features of the ground-state structure. This result parallels the inspection of the molecular orbitals close to the HOMO and LUMO (not reported) of N2B, showing that they remain almost confined to phenyl and one (of two) naphthyl. This last result explains the similarity between the two compounds. Furthermore, the slight shift of the ^1B_b band of N2B, with respect to N1B, supports the fact that a more extended longitudinal delocalization is not induced by the second naphthyl group.

Both of the energy gaps between the considered excited states and S_0 are similar and fall in the broad fluorescence band, experimentally detected at about 350 nm, confirming the goodness of these structures. In N1B and N2B, the major rearrangement in both excited states involves the dihedral angle between the aromatic rings that assumes values equal to about 45, 0, and 31° for S_0, S_1, and S_2 states, respectively.

Furthermore, as previously reported, the major contribution to the Herzberg−Teller terms, for the couplings between S_0 and S_1 in N1B,[7c] is due to the normal coordinate related to the torsion of the two rings. The torsion of this dihedral angle is also needed to transit between the minimum structures of S_0 and S_1. Analogously, a torsion around the same dihedral angle is involved in the structural rearrangement needed to obtain the S_2 minimum structure from S_0.

We hypothesize that the efficiency of coupling between S_1 and S_2, involving the torsion around ϕ, is at the basis of the occurrence of the biexponential decay time. The presence of a naphthyl group in position three likely changes the features of this coupling, and the two species differently contribute, in N1B and N2B, by varying the experimental conditions.

Furthermore, we have shown that in the region without the Stokes shift the fluorescence is almost due to the species with the shorter fluorescence decay time. The major part of Stoke-shift is associated with the ϕ torsion that can be fully explored in the ground state (see above). As a result, a small portion of absorption can take place from molecules with the excited-state geometry that does not undergo significant rearrangements. The evidence that, under this condition, practically only one fluorescence decay time is detected suggests that in the excited state, the coupling between different electronic levels, without ϕ rearrangements, is depleted and a monoexponential decay time is observed.

This evidence corroborates the hypothesis that the biexponential decay is a consequence of the coupling between different electronic levels. Interestingly, the involvement of the S_2 state, leading to a biexponential decay, was already observed in a similar system.[25] The authors, in that case, concluded that this is favored when S_1 and S_2 states are close in energy but different from a conformational point of view, as in our case.

Conclusions

N1B, N2B, and N3B, for their high quantum yields and stabilities, constitute a versatile scaffold for applications where the emission properties play a role (i.e., OLED). In this article, the spectroscopic and computational data are reported to elucidate their photophysical properties.

The addition of a second naphthyl group to N1B, leading to N2B, perturbs the electronic states, as can be deduced from absorption and steady-state fluorescence spectra. Surprisingly, in all investigated properties, no differences are detected between N2B and N3B.

All investigated compounds show biexponential decays that do not derive from the heterogeneity of the ground state (i.e., aggregates or conformers) but from the excited state rearrangements involving S_1 and S_2.

A combined computational approach, based on ab initio and semiempirical methods, correctly predicts the spectroscopic features of the investigated compounds. Minimized structures have also been obtained for S_0, S_1, and S_2 states that differ mainly by the value of the dihedral angles between the aromatic rings. According to our hypothesis, the efficiency of the nonradiative decay from S_2 to S_1 can lead to different emitting states.

Acknowledgment. This work was supported by MIUR. We thank Mr. E. Fresch for his technical support.

References and Notes

(1) Simpson, C. D.; Mattersteig, G.; Martin, K.; Gherghel, L.; Bauer, R. E.; Räder, H. J.; Müllen, K. *J. Am. Chem. Soc.* **2004**, *126*, 3129.

(2) Huff, B. E.; Koenig, T. M.; Mitchell, D.; Staszak, M. A. *Org. Synth.* **1998**, *75*, 53.

(3) (a) Su, S.-J.; Chiba, T.; Takeda, T.; Kido, J. *Adv. Mater.* **2008**, 1–6. (b) Zhao, Z.; Xu, X.; Wang, H.; Lu, P.; Yu, G.; Liu, Y. *J. Org. Chem.* **2008**, *73*, 594.

(4) Bonvallet, P. A.; Breitkreuz, C. J.; Kim, Y. S.; Todd, E. M.; Traynor, K.; Fry, C. G.; Ediger, M. D.; MacMahon, R. J. *J. Org. Chem.* **2007**, *72*, 10051.

(5) (a) Tagliatesta, P.; Floris, B.; Galloni, P.; Leoni, A.; D'Arcangelo, G.*Inorg. Chem.* **2003**, *42*, 7701. (b) Elakkari, E.; Floris, B.; Galloni, P.; Tagliatesta, P. *Eur. J. Org. Chem.* **2005**, 889. (c) Tagliatesta, P.; Elakkari, E.; Leoni, A.; Lembo, A.; Cicero, D. *New J. Chem.* **2008**, *32*, 1847.

(6) (a) Whitaker, C. M.; McMahon, R. J. *J. Phys. Chem.* **1996**, *100*, 1081–1090. (b) Plazek, D. J.; Magill, J. H.; Echeverria, I.; Chai, I.-C. *J. Chem. Phys.* **1999**, *110*, 10445.

(7) (a) Holloway, H. E.; Nauman, R. V.; Wharton, J. H. *J. Phys. Chem.* **1968**, *72*, 4468. (b) Holloway, H. E.; Nauman, R. V.; Wharton, J. H. *J. Phys. Chem.* **1968**, *72*, 4474. (c) Gustav, K.; Storch, M. *Struct. Chem.* **1990**, *2*, 589–594. (d) Gustav, K.; Kempka, U.; Sühnel, J. *Chem. Phys. Lett.* **1980**, *71*, 280.

(8) (a) Monguzzi, A.; Tubino, R.; Meinardi, F. *Phys. Rev. B* **2008**, *77*, 155122. (b) Monguzzi, A.; Mézyk, J. F.; Tubino, R.; Meinardi, F. *Phys. Rev. B* **2008**, *78*, 195112.

(9) Beechem, J. M.; Gratton, E.; Ameloot, M.; Knutson, J. R.; Brand. L. In *Topics in Fluorescence Spectroscopy: Principles*; Lakowicz, J. R., Ed.; Plenum Press: New York, 1991; Vol. 2, p 241.

(10) Lakowicz, J. R. In: *Principles of Fluorescence Spectroscopy*; Kluwer Academy Publishers: New York, 1999.

(11) Pispisa, B.; Mazzuca, C.; Palleschi, A.; Stella, L.; Venanzi, M.; Wakselman, M.; Mazaleyrat, J. P.; Rainaldi, M.; Formaggio, F.; Toniolo, C. *Chem.—Eur. J.* **2003**, *9*, 2.

(12) (a) Konopasek, I.; Kvasnicka, P.; Herman, P.; Linnertz, H.; Obsil, T.; Vecer, J.; Svobodova, J.; Strzalka, K.; Mazzanti, L.; Amler, E. *Chem. Phys. Lett. B* **1998**, *293*, 429. (b) Donzel, B.; Gauduchon, P.; Wahl, P. *J. Am. Chem. Soc.* **1974**, *96*, 801.

(13) Eaton, D. F. *Pure Appl. Chem.* **1988**, *60*, 1107.

(14) Venanzi, M.; Bocchinfuso, G.; Palleschi, A.; Abreu, A. S.; Ferreira, P. M. T.; Queiroz, M-J. R. P. *J. Photochem. Photobiol., A* **2005**, *170*, 181.

(15) (a) Karpovic, D. S.; Blanchard, G. J. *J. Phys. Chem.* **1995**, *99*, 3951–3958. (b) Nakajima, A. *Bull. Chem. Soc. Jpn.* **1971**, *44*, 3272.

(16) (a) Foresman, J. B.; Head-Gordon, M.; Pople, J. A. *J. Phys. Chem.* **1992**, *96*, 135. (b) Schlegel, H. B.; Foresman, J. B. *NATO Adv. Sci. Inst. Ser., Ser. C* **1993**, 11–20.

(17) (a) Anderson, W. P.; Edwards, W. D.; Zerner, M. C. *Inorg. Chem.* **1986**, *25*, 2728. (b) Anderson, W. P.; Cundari, T. R.; Drago, R. S.; Zerner, M. C. *Inorg. Chem.* **1990**, *29*, 1. (c) Kotzian, M.; Rosch, N.; Schroeder, H.; Zerner, M. C. *J. Am. Chem. Soc.* **1989**, *111*, 7687.

(18) Frisch, M. J.; Trucks, G. W.; Schlegel, H. B.; Scuseria, G. E.; Robb, M. A.; Cheeseman, J. R.; Montgomery, J. A., Jr.; Vreven, T.; Kudin, K. N.; Burant, J. C.; Millam, J. M.; Iyengar, S. S.; Tomasi, J.; Barone, V.; Mennucci, B.; Cossi, M.; Scalmani, G.; Rega, N.; Petersson, G. A.; Nakatsuji, H.; Hada, M.; Ehara, M.; Toyota, K.; Fukuda, R.; Hasegawa, J.; Ishida, M.; Nakajima, T.; Honda, Y.; Kitao, O.; Nakai, H.; Klene, M.; Li, X.; Knox, J. E.; Hratchian, H. P.; Cross, J. B.; Bakken, V.; Adamo, C.; Jaramillo, J.; Gomperts, R.; Stratmann, R. E.; Yazyev, O.; Austin, A. J.; Cammi, R.; Pomelli, C.; Ochterski, J.; Ayala, P. Y.; Morokuma, K.; Voth, G. A.; Salvador, P.; Dannenberg, J. J.; Zakrzewski, V. G.; Dapprich, S.; Daniels, A. D.; Strain, M. C.; Farkas, O.; Malick, D. K.; Rabuck, A. D.; Raghavachari, K.; Foresman, J. B.; Ortiz, J. V.; Cui, Q.; Baboul, A. G.; Clifford, S.; Cioslowski, J.; Stefanov, B. B.; Liu, G.; Liashenko, A.; Piskorz, P.; Komaromi, I.; Martin, R. L.; Fox, D. J.; Keith, T.; Al-Laham, M. A.; Peng, C. Y.; Nanayakkara, A.; Challacombe, M.; Gill, P. M. W.; Johnson, B. G.; Chen, W.; Wong, M. W.; Gonzalez, C.; Pople, J. A. *GAUSSIAN 03*, revision C.02; Gaussian, Inc.: Wallingford, CT, 2004.

(19) Jaffè, H. H.; Orchin, M. In *Theory and Application of UV Spectroscopy*; Wiley and Sons: New York, 1962.

(20) Mazzuccato, U.; Momicchioli, F. *Chem. Rev.* **1991**, *91*, 1679.

(21) (a) Sugimoto, M.; Sakaki, S.; Sakanoue, K.; Newton, M. D. *J. Appl. Phys.* **2001**, *90*, 6092. (b) Liu, X.; Ju, H.; Zhao, X.; Tao, X.; Bian, W.; Jiang, M. *J. Chem. Phys.* **2006**, *124*, 174711.

(22) Zachariasse, K. A.; Druzhinin, S. I.; Galievsky, V. A.; Kovalenko, S.; Senyushkina, T. A.; Mayer, P.; Noltemeyer, M.; Boggio-Pasqua, M.; Robb, M. A. *J. Phys. Chem. A* **2009**, *113*, 2693.

(23) (a) Stella, L.; Mazzuca, C.; Venanzi, M.; Palleschi, A.; Didonè, M.; Formaggio, F.; Toniolo, C.; Pispisa, B. *Biophys. J.* **2004**, *86*, 936. (b) Venanzi, M.; Bocchinfuso, G.; Gatto, E.; Palleschi, A.; Stella, L.; Formaggio, F.; Toniolo, C. *ChemBioChem* **2009**, *10*, 91. (c) Pispisa, B.; Mazzuca, C.; Palleschi, A.; Stella, L.; Venanzi, M.; Formaggio, F.; Toniolo, C.; Mazaleyrat, J. P.; Wakselman, M. *J. Fluoresc.* **2003**, *13*, 139.

(24) Ladokhin, A. S.; White, S. H. *Biophys. J.* **2001**, *81*, 1825.

(25) Aloisi, G. G.; Elisei, F.; Latterini, L.; Marconi, G.; Mazzuccato, U. *J. Photochem. Photobiol., A* **1997**, *105*, 289.

(26) (a) Rettig, W.; Maus, M. In *Conformational Analysis of Molecules in Excited States*; Waluk, J., Ed; Wiley-VCH: New York, 2000; p 57. (b) Bartocci, G.; Spalletti, A.; Mazzuccato, U. In *Conformational Analysis of Molecules in Excited States*; Waluk, J., Ed; Wiley-VCH: New York, 2000; p 237.

(27) Grein, F. *THEOCHEM* **2003**, *624*, 23.

JP905059V